$NdTe_2$[18] may be described as a tricapped trigonal prism.

The sulfur atoms in Gd_2S_3 are all coordinated by five gadolinium atoms. A trigonal-bipyramidal arrangement is found for S(1) with average S–Gd distances of 2.90 Å, and S(2) and S(3) are in square pyramids with average S–Gd distances of 2.85 and 2.83 Å, respectively. Figure 2 shows the coordination polyhedra associated with each atom. The S–S distances are all greater than 3.40 Å except for one of 3.04 Å between S(2) and S(3) centered around the point 0.37, 0.48, $^3/_4$ in Figure 1. This short S(2)–S(3) distance represents a polyhedral edge shared between two Gd(1) polyhedra and one Gd(2) polyhedron and is the only edge shared by more than two of the gadolinium polyhedra. There are, however, no unusually short Gd–Gd distances in the structure, the shortest being one of 3.888 Å between Gd(1) and Gd(2). This is consistent with the magnetic data[7] which indicate very weak interactions between gadolinium atoms. For Gd_2S_3 there are no magnetic transitions down to 4.2°K, the Curie–Weiss constant (θ) is −8°K, and the observed moment of 7.94 ± 0.01 BM is in excellent agreement with the calculated value[19] of 7.94 BM.

Recently, a structure for monoclinic Ho_2S_3 has been reported[20] which contains half of the Ho in octahedral and half in sevenfold coordination. Thus the coordination of the rare earth is showing a general tendency to increase as the size of the rare earth increases, going from six in the corundum type, through mixed six and seven in the monoclinic type, to mixed seven and eight in the orthorhombic type.

(18) R. Wang, H. Steinfink, and W. F. Bradley, *Inorg. Chem.*, **5**, 142 (1966).

(19) J. H. Van Vleck, "The Theory of Electric and Magnetic Susceptibilities," Oxford University Press, London, 1944.

(20) J. G. White, P. N. Yocom, and S. Lerner, *Inorg. Chem.*, **6**, 1872 (1967).

CONTRIBUTION NO. 1411 FROM THE CENTRAL RESEARCH DEPARTMENT, EXPERIMENTAL STATION, E. I. DU PONT DE NEMOURS AND COMPANY, WILMINGTON, DELAWARE 19898

Magnetic, Mössbauer, and Structural Studies on Three Modifications of $FeMoO_4$

BY A. W. SLEIGHT, B. L. CHAMBERLAND, AND J. F. WEIHER

Received January 4, 1968

Three modifications of $FeMoO_4$ have been characterized by magnetic susceptibility, Mössbauer effect, and X-ray studies. The low-temperature, low-pressure form, α-$FeMoO_4$, is isostructural with low-temperature $NiMoO_4$ and $CoMoO_4$. The high-temperature, low-pressure form, β-$FeMoO_4$, is isostructural with $MnMoO_4$ and $MgMoO_4$ and exists metastably at room temperature when quenched from above 600°. The high-pressure form, $FeMoO_4$-II, represents a triclinic distortion of the monoclinic $NiWO_4$-type structure. Magnetic and Mössbauer results indicate high-spin divalent iron to be present in all three modifications. Antiferromagnetic interactions in $FeMoO_4$-II lead to magnetic order below 45°K.

Introduction

At least two forms of $FeMoO_4$ are known to exist. A low-pressure modification, α-$FeMoO_4$, was first prepared by Schultze[1] as monoclinic prisms from a fused-salt reaction. This product has also been reported by others,[2-6] and the X-ray diffraction powder pattern has been presented.[2,6,7] Its structure has generally been believed to be different from those of the normal (STP) forms of all other $A^{2+}Mo^{6+}O_4$-type molybdates (where A may be Mg, Mn, Co, Ni, Zn, and Cu).[8-10] Abrahams[11] states that normal (STP) $FeMoO_4$ is probably triclinic. Young and Schwartz[12] have reported a high-pressure modification, $FeMoO_4$-II, which they found to be structurally related to $NiWO_4$.

The purpose of this investigation was to identify the various modifications of $FeMoO_4$ and to compare their properties. It was of particular interest to determine if the reportedly unique structure for α-$FeMoO_4$ might be due to an unusual valence combination, *i.e.*, Fe^{3+}-$Mo^{5+}O_4$, instead of $Fe^{2+}Mo^{6+}O_4$.

Experimental Section

All forms of $FeMoO_4$ could be prepared from an appropriate mixture of Fe_2O_3, MoO_3, and Mo or Fe_2O_3, MoO_3, and Fe. The reactants, obtained from Johnson, Matthey & Co., were all at least 99.99% pure. Both low-pressure forms of $FeMoO_4$ were prepared by heating the intimately mixed reactants in evacuated platinum or silica tubes at 900–1000° for 1–2 days. Depending on the cooling rate, the product was α-$FeMoO_4$, β-$FeMoO_4$, or a mixture of these two forms. α-$FeMoO_4$ was also prepared by mixing stoichiometrically solutions of $FeCl_2$ and Na_2MoO_4 at about 100° and then drying the precipitate at 400° under vacuum.

(1) H. Schultze, *Ann.*, **126**, 49 (1863).
(2) Yu. D. Kozmanov, *Zh. Fiz. Khim.*, **31**, 1861 (1957).
(3) A. N. Zelikman and L. V. Belyaevskaya, *Zh. Prikl. Khim.*, **27**, 1151 (1954); **29**, 11 (1956).
(4) A. N. Zelikman, *Zh. Neorgan. Khim.*, **1**, 2778 (1956).
(5) Yu. D. Kozmanov and T. A. Ugol'nikova, *ibid.*, **3**, 1267 (1958).
(6) W. Jäger, A. Rahmel, and K. Becker, *Arch. Eisenhuttenw.*, **30**, 435 (1959).
(7) F. Corbet, R. Stefani, J. C. Merlin, and C. Eyrand, *Compt. Rend.*, **246**, 1696 (1958).
(8) G. W. Smith and J. A. Ibers, *Acta Cryst.*, **19**, 269 (1965).
(9) G. W. Smith, *ibid.*, **15**, 1054 (1962).
(10) S. C. Abrahams and J. M. Reddy, *J. Chem. Phys.*, **43**, 2533 (1965).
(11) S. C. Abrahams, *ibid.*, **46**, 2052 (1967).
(12) A. P. Young and C. M. Schwartz, *Science*, **141**, 348 (1963).

In hydrothermal experiments the reactants were sealed in pressure-collapsible gold tubes with 1 ml of water to about 5 g of the reactants. A supporting pressure of 3 kbars was used. High-pressure experiments (above 3 kbars) were carried out using a tetrahedral anvil apparatus previously described.[13] In these experiments the container was gold or platinum.

Single crystals of α-$FeMoO_4$ and $FeMoO_4$-II suitable for X-ray studies (Table I) were found in preparations described above. Precession photographs established that the space group of α-$FeMoO_4$ was C2, Cm, or C2/m, while $FeMoO_4$-II was found to be triclinic. Cell dimensions are given in Table II. Powder patterns of all three modifications were obtained with a Hägg–Guinier camera using strictly monochromatic Cu $K\alpha_1$ radiation and an internal standard of KCl (a = 6.2931 Å). Qualitative intensities (peak height) were obtained with a powder diffractometer. High-temperature powder patterns were obtained with a Materials Research Corp. high-temperature camera using an evacuated chamber.

TABLE I

POWDER DIFFRACTION DATA FOR THE VARIOUS POLYMORPHS OF $FeMoO_4$[a]

α-FeMoO4					β-FeMoO4					FeMoO4-II				
h k l	d obs	d calc	I/I0 calc	I/I0 obs	h k l	d obs	d calc	I/I0 calc	I/I0 obs	h k l	d obs	d calc	I/I0 calc	I/I0 obs
1 1 0	6.329	6.330	74	75	1 1 0	6.807	6.807	72	65	0 1 0	5.604	5.607	3	5
1 1 1	5.55n	5.557	6	5	1 1 1	--	--	8	5	1 0 0	4.703	4.705	34	40
2 0 1	4.750	4.751	11	10	2 0 1	4.664	4.665	9	5	0 1 1	3.795	3.755	26	20
1 1 1	4.139	4.138	2	2	1 1 1	--	--	2		0 1 1	3.710	3.710	95	70
0 2 1	3.769	3.770	13	15	2 0 1	3.866	3.866	12	15	1 1 0	3.703	3.702	56	40
2 0 $\bar{2}$	3.541	3.545	16	20	2 0 1	3.547	3.547	5	10	1 1 0	3.558	3.558	58	75
1 1 2	3.539	3.541	34	40	2 0 0	3.403	(3.403	100	113	1 1 1	2.977	2.978	95	90
0 0 2	3.469	3.468	17	20	2 0 $\bar{2}$		(3.393	13		1 1 1	2.947	2.946	100	80
2 0 1	3.324	3.321	5	5	1 1 $\bar{2}$	3.303	3.303	23	20	1 $\bar{1}$ 1	2.893	2.893	95	100
2 2 0	3.164	3.165	100	100	2 0 $\bar{2}$	3.256	3.256	12	10	1 1 1	2.888	2.889	87	80
3 1 0)	2.832	(2.831	11	8	3 1 1	--	--	8	--	0 2 0	2.848	2.848	26	30
1 3 0)		(2.830	8)		1 3 0	--	--	8	--	1 2 0	--	--	5	--
3 1 $\bar{2}$	2.788	2.791	23	25	1 1 2	2.807	2.807	21	20	0 0 1	2.480	2.481	33	40
2 2 $\bar{2}$	2.778	2.779	23	25	0 2 2	2.751	2.751	17	10	0 0 2	2.479	2.478	47	60
0 2 2	2.754	2.755	21	20	2 2 $\bar{2}$	2.675	2.676	17	25	0 2 1	2.456	2.456	33	20
1 1 2	2.745	2.745	24	20	3 1 $\bar{2}$	2.672	2.671	17	15	1 $\bar{2}$ 0	--	--	5	--
4 0 $\bar{2}$	2.375	2.375	5	10	2 0 2	--	--	5	--	2 0 0	2.352	2.352	65	50
1 3 $\bar{2}$	2.353	2.353	12	10	4 0 0	2.469	2.469	10	10	1 2 $\bar{1}$	--	--	3	--
2 0 2	2.333	2.333	5	10	0 4 0	2.349	2.349	8	10	1 2 1	--	--	12	--
4 0 0)	2.230	(2.232	91	15	1 3 $\bar{2}$	2.349	2.349	10	5	1 0 $\bar{2}$	2.154	2.154	14	20
0 4 0)		(2.228	8)		4 0 $\bar{2}$	2.332	2.332	4	5	1 $\bar{2}$ 1	2.148	2.148	31	15
2 2 3	2.205	2.205	2	2	3 3 0	2.269	2.269	48	35	1 2 1	--	--	2	--

[a] The reflections given are, in each case, the first 22 for which $(I/I_0)_{calcd}$ is 2 or greater.

TABLE II

CELL DIMENSIONS OF SOME $AMoO_4$ COMPOUNDS[a]

Compound	Parameters, Å			Angle,[b] deg	V, Å³
	a	b	c		
α-$NiMoO_4$	9.555	8.745	7.693	113.62	588.7
α-$CoMoO_4$	9.666	8.854	7.755	113.82	607.2
α-$FeMoO_4$	9.805	8.950	7.660	114.05	613.9
β-$FeMoO_4$	10.290	9.394	7.072	106.31	656.1
β-$NiMoO_4$	10.13	9.28	7.02	107.2	630
β-$CoMoO_4$	10.21	9.31	7.01	106.4	639
$MgMoO_4$	10.278	9.291	7.027	106.90	642.1
$MnMoO_4$	10.469	9.516	7.143	106.28	683.1
$FeMoO_4$-II[c]	4.7078	5.7006	4.9443	90.67 (α) 90.27 (β) 87.68 (γ)	528.3/4
$FeMoO_4$-II[d]	4.9443	5.7006	4.7078	92.32 (α) 90.27 (β) 89.33 (γ)	

[a] Errors are about ±1 in the last significant figure. [b] β unless otherwise stated. [c] Cell related to $NiWO_4$. [d] Conventional reduced cell.

The cell dimensions of all three forms of $FeMoO_4$ as well as $MgMoO_4$, $MnMoO_4$, and α-$NiMoO_4$ were refined by least squares using Guinier camera powder data. The calculated intensities (Table I) were obtained using the relationship $I = F^2MLp$ where Lp is the Lorentz and polarization factors, M is the multiplicity, and F is the structure factor. Absorption was neglected since it is nearly constant with θ for the diffractometer method. The structure factors were calculated assuming the published positional parameters of $CoMoO_4$,[8] $MnMoO_4$,[10] and $NiWO_4$[14] for α-$FeMoO_4$, β-$FeMoO_4$, and $FeMoO_4$-II, respectively. The structure factors calculated for α-$FeMoO_4$ and β-$FeMoO_4$ were found to be nearly identical with the published structure factors for $CoMoO_4$ and $MnMoO_4$, respectively, as expected. The ratio of parameters to observations was considered to be too great for meaningful refinements of the powder data; consequently, no R's were calculated.

Dta experiments were performed with a Du Pont 900 differential thermal analyzer. The heating rate was 15°/min, and a protective argon atmosphere was used.

Electrical resistivity was measured on α-$FeMoO_4$ and $FeMoO_4$-II. A standard four-probe technique was used on a single crystal of $FeMoO_4$-II over a temperature range of 133–298°K. Crystals of α-$FeMoO_4$ were too small for this technique; consequently, measurements were made on a powder compact using two probes.

The magnetic susceptibilities of α-$FeMoO_4$ and $FeMoO_4$-II were measured by the conventional Faraday method using a Cahn RG microbalance, a field gradient ($H\partial H/\partial x$) of the order of 10^7 Oe^2/cm at 8000 Oe, and $HgCo(CNS)_4$ as a calibrant.

The Mössbauer spectra were observed with an NSEC-AM-1 spectrometer utilizing a Reuter–Stokes RG-30 Kr–N_2-filled proportional counter for γ detection, RIDL 31-24A and 33-13A preamplifier and single-channel analyzer, and a Nuclear Data ND-180 for the multichannel analyzer. The source was 2-mCi Co^{57} in Cu foil which was kept at the same temperature as the adsorber. Velocity scans were calibrated by means of the quadrupole splitting of a polycrystalline sample of $Na_2Fe(CN)_5NO \cdot 2H_2O$, which exhibits an isomeric shift relative to the source of −0.490 ± 0.005 mm/sec. Peak positions were determined by computer fit using a least-squares minimization assuming Lorentzian line shape.

Results

Polymorphic Transitions.—Three different modifications of $FeMoO_4$ were obtained. In an effort to be consistent with the current usage, the following terminology has been adopted: low-temperature, low-pressure form, α-$FeMoO_4$; high-temperature, low-pressure form, β-$FeMoO_4$; and high-pressure form, $FeMoO_4$-II. From the volumes in Table II, the following densities (STP) are calculated: β-$FeMoO_4$, 4.368; α-$FeMoO_4$, 4.668; $FeMoO_4$-II, 5.425 g/cm^3. This is, of course, the trend which would be expected. The low-temperature form is 6.8% denser than the high-temperature form, and the high-pressure form is 24.2% denser than the β form.

Whether the α or β form of low-pressure $FeMoO_4$ is obtained at room temperature depends on the cooling rate from about 600°. Quick cooling (600° to room temperature in about 1 sec) produces mostly β-$FeMoO_4$, whereas slower cooling, *e.g.*, about 100°/min, gives mostly α-$FeMoO_4$. Usually, one form is slightly contaminated with the other. However, all traces of β-$FeMoO_4$ may be removed from α-$FeMoO_4$ by sufficient grinding at room temperature or by cooling to 78°K. It was also possible to prepare α-$FeMoO_4$ below 600° by precipitation. A powder pattern at 78°K showed that α-$FeMoO_4$ does not transform to another form on cooling to this temperature.

The transformation of α- to β-$FeMoO_4$ was followed by dta and high-temperature X-ray diffraction. A broad endotherm was found at about 400° by dta on heating α-$FeMoO_4$. High-temperature X-ray diffraction confirmed that α-$FeMoO_4$ begins to transform to β-$FeMoO_4$ at about 400°, and the β form was found to

(13) T. A. Bither, J. L. Gillson, and H. S. Young, *Inorg. Chem.*, **5**, 1559 (1966).

(14) R. O. Keeling, *Acta Cryst.*, **10**, 209 (1957).

remain stable to at least 1000°. A sharp endotherm at 1115 ± 5° was presumed to be the melting point of β-$FeMoO_4$. Apparently, β-$FeMoO_4$ melts congruently because samples quenched from the melt were β or α type with no impurities detected by X-ray.

The transition of β- to α-$FeMoO_4$ can be quite violent with crystals of β-$FeMoO_4$ actually exploding on transforming to α-$FeMoO_4$. The resulting α-$FeMoO_4$ is fine powder or crystal fragments less than ~0.1 mm in size. Such violent transitions have also been reported[15] for $CoMoO_4$ and $NiMoO_4$.

Conditions similar to those reported by Young and Schwartz[12] were first used to prepare $FeMoO_4$-II. However, while this form is readily prepared at 60 kbars and 900°, α- or β-$FeMoO_4$ was obtained at about 10 kbars and 900° under anhydrous conditions. Hydrothermally, $FeMoO_4$-II was obtained at 3 kbars and 700°. Preparation of $FeMoO_4$-II from Fe_2O_3, MoO_3, and Fe at 65 kbars and 900°, from α-$FeMoO_4$ at 65 kbars and 900°, and from Fe_2O_3, MoO_3, and Fe at 3 kbars and 700° hydrothermally all gave X-ray Guinier patterns which appeared identical. Furthermore, the dta curves and magnetic susceptibility data for these various products were the same within experimental error. Marshall[16] has recently reported the growth of $FeMoO_4$-II crystals hydrothermally at 480° and pressures greater than 650 bars. These conditions were repeated here, and the product was found to be identical with our preparations of $FeMoO_4$-II. It appears, therefore, that there is no monoclinic $FeMoO_4$-II at STP as has been reported.[12,16] On heating $FeMoO_4$-II, sharp endotherms were found at 620 ± 5° and at 1115 ± 5° (melting point of β-$FeMoO_4$). High-temperature X-ray diffraction showed that $FeMoO_4$-II transformed to β-$FeMoO_4$ at about 620°.

Structural Studies.—Despite several reports to the contrary, we find the X-ray powder pattern of α-$FeMoO_4$ to be very similar to those of α-$NiMoO_4$ and α-$CoMoO_4$. This observation has also been made by Kozmanov.[2] The crystal structure of α-$CoMoO_4$ has been solved and refined by Smith and Ibers,[8] and α-$NiMoO_4$ is known to be isotypic with α-$CoMoO_4$.[9] Our single-crystal data on α-$FeMoO_4$ are consistent with the space group C2/m reported for α-$CoMoO_4$. Furthermore, the failure to observe a piezoelectric effect with a very sensitive apparatus[17] supports space group C2/m over C2 or Cm. The unit cell dimensions of α-$FeMoO_4$ are very similar to those of α-$CoMoO_4$ and α-$NiMoO_4$ (Table III). The observed d spacings and intensities of a powder pattern of α-$FeMoO_4$ are compared with the calculated values in Table I. The intensities were calculated assuming the published coordinates of α-$CoMoO_4$.[8] There is little doubt that α-$FeMoO_4$, α-$CoMoO_4$, and α-$NiMoO_4$ are all isotypic although it would still be desirable to refine the structures of α-$FeMoO_4$ and α-$NiMoO_4$.

The powder pattern of β-$FeMoO_4$ was successfully indexed assuming it to be of the $MnMoO_4$ type. The observed d spacings and intensities are compared with calculated values in Table I. The intensities were calculated assuming the published atomic coordinates for $MnMoO_4$.[10] Since we have found[18] that $MgMoO_4$, β-$CoMoO_4$, and β-$NiMoO_4$ are isotypic with $MnMoO_4$, these cell dimensions are also given in Table II.

TABLE III
MAGNETIC SUSCEPTIBILITY PARAMETERS

Phase	θ, °K	μ, BM[a]	$T_{\chi max}$, °K	$10^3\chi_{FeMoO_4}$ (300°K)[b]
α-$FeMoO_4$	+40 ± 5	5.25 ± 0.05	30 ± 5	13.2 ± 0.2
$FeMoO_4$-II	−105 ± 5	5.78 ± 0.05	45 ± 5	10.3 ± 0.2

[a] Total magnetic moment determined from slope of the Curie–Weiss region. [b] Observed molar susceptibility corrected for ion-core diamagnetism ≈0.07 × 10^{-3}/mole.

The crystal structure of $FeMoO_4$-II has been reported to be of the $NiWO_4$ type.[12] Although this is basically correct, single-crystal photographs and Guinier patterns showed the symmetry to be triclinic. The failure to observe a piezoelectric effect with a very sensitive apparatus[17] supports space group $P\bar{1}$ over P1. The observed d spacings and intensities were calculated assuming the published atomic coordinates for $NiWO_4$ and space group $P\bar{1}$. The cell dimensions for $FeMoO_4$-II are given twice in Table II. The first cell is easily related to the $NiWO_4$ cell, and the indices in Table I correspond to this cell. The second cell is the conventional reduced cell.

Magnetic Studies.—The magnetic susceptibilities of powder samples of both α-$FeMoO_4$ and $FeMoO_4$-II exhibit Curie–Weiss behavior at higher temperatures (Figure 1). The susceptibility of both phases was independent of field over 1000–8000 Oe at 4.2 and 78°K. The magnetic parameters of these two phases are summarized in Table III.

The reciprocal magnetic susceptibility *vs.* temperature curve for the high-pressure phase is typical of a system with antiferromagnetic interactions. This is indicated by both the negative Weiss constant, $\theta = -105$°K, and the minimum in the reciprocal susceptibility at about 45°K. The total magnetic moment per $FeMoO_4$ unit, $\mu = 5.78$ BM, in the general case is a combination of contributions from both iron and molybdenum.

Four possibilities were considered: (1) ferrous high-spin iron, (2) ferric high-spin iron, (3) ferric low-spin iron, (4) zero moment from Mo^{5+}. Estimates of the total moment for these cases can be determined, $\mu = \sqrt{\mu_1^2 + \mu_2^2}$, from the expected atomic contributions in Table IV.[19]

For the first case, ferrous iron, the observed moment must arise solely from the iron because the d^0 configuration of the Mo^{6+} can contribute no moment. Since the observed moment, 5.78 BM, lies at the upper end of the expected range for high-spin ferrous iron, the nominal valence distribution, $Fe^{2+}Mo^{6+}O_4$, is one

(15) Y. Trambouze, Y. Colleuille, and T. H. The, *Compt. Rend.*, **242**, 497 (1956).
(16) D. J. Marshall, *J. Mater. Sci.*, **2**, 294 (1967).
(17) R. J. Blume, *Rev. Sci. Instr.*, **32**, 598 (1961).
(18) A. W. Sleight and B. L. Chamberland, to be submitted for publication.
(19) B. N. Figgis and J. Lewis, *Progr. Inorg. Chem.*, **6**, 37 (1964).

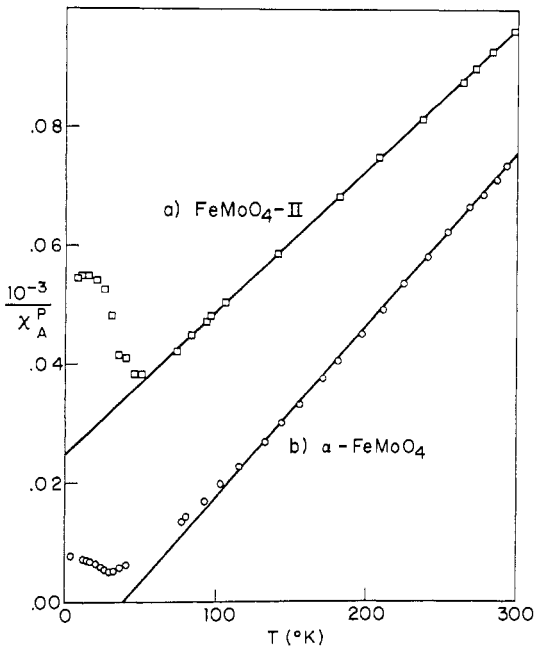

Figure 1.—Magnetic susceptibility of $FeMoO_4$: (a) high-pressure phase, $FeMoO_4$-II; (b) low-pressure phase, α-$FeMoO_4$.

TABLE IV
EXPECTED ATOMIC MOMENTS IN OCTAHEDRAL SITES[a]

Ion	μ (low spin), BM	μ (high spin), BM
Fe^{2+} (d^6)	0	4.9–5.8
Fe^{3+} (d^5)	1.7–2.5	5.9–6.0
Mo^{6+} (d^0)	0	0
Mo^{5+} (d^1)	1.5–2.0	1.5–2.0

[a] Compiled from the data survey of Figgis and Lewis.[19]

possible interpretation. In the second and third cases, $Fe^{3+}Mo^{5+}O_4$ with high- and low-spin iron, the estimated total moments, μ = 6.1–6.30 and 2.3–3.2 BM, respectively, are in poor agreement with the observed moment, and so these cases are rejected. If, however, a Mo^{5+} lattice were antiferromagnetically ordered at room temperature and below, or if the electron associated with Mo^{5+} were delocalized, it would contribute essentially zero moment, so that the estimated moment for case four is 5.9–6.0 BM. This is in sufficiently close agreement with the observed 5.78 BM to be considered as a second possibility. Thus the magnetic data for $FeMoO_4$-II indicate that the iron must be in a high-spin state but do not clearly distinguish between ferrous and ferric iron.

The temperature dependence of the magnetic susceptibility of the α-$FeMoO_4$ phase is anomalous. The positive Weiss constant θ = +40°K suggests a ferromagnetic interaction, but the minimum in the reciprocal susceptibility at about 30°K suggests either antiferromagnetic order or a change in spin state. An analysis similar to that for the high-pressure phase for the total moment at higher temperatures, μ = 5.25 BM, strongly indicates $Fe^{2+}Mo^{6+}O_4$.

Mössbauer-Effect Studies.—The observed Mössbauer effect for α-$FeMoO_4$ exhibits a two-line pattern at 297 and 78°K (Figure 2). This is interpreted as

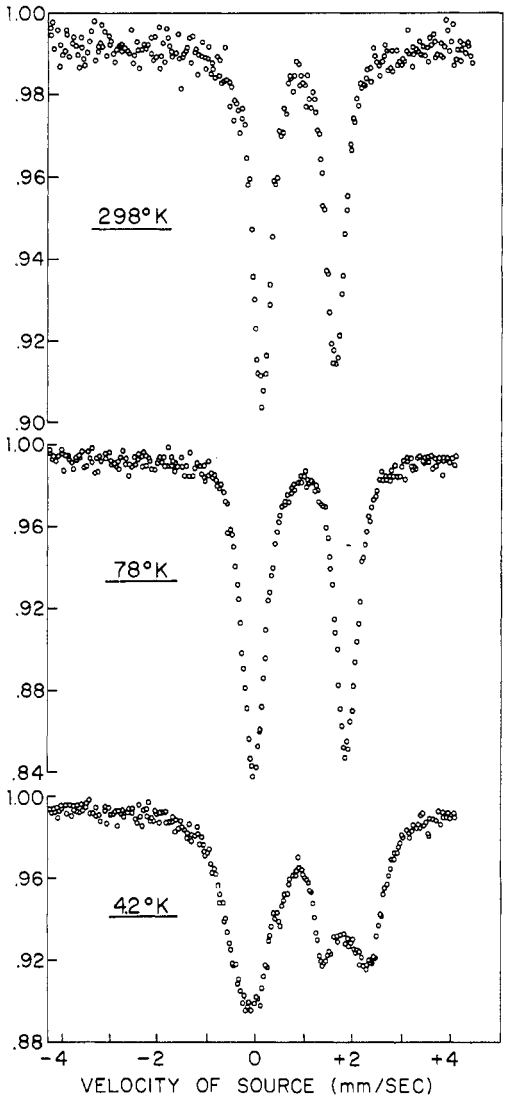

Figure 2.—Mössbauer effect of α-$FeMoO_4$.

arising from a single (within experimental error and overlap considerations) quadrupole split transition. Visual inspection of the spectrum at 4.2°K indicates three or more lines which are broader than those at higher temperatures. This can be interpreted either as two overlapping quadrupole pairs or as a partially unresolved six-line magnetic hyperfine pattern for which the effective internal field is small and comparable in magnitude to the quadrupole splitting. In an attempt to resolve this ambiguity, a further spectrum was obtained on α-$FeMoO_4$ at 2.5°K. This spectrum was essentially identical with that obtained at 4.2°K.

Above the Neel point $FeMoO_4$-II exhibits a two-line pattern (Figure 3a) arising from quadrupole split transition. Below the Neel point, 4.2°K (Figure 3b), a well-resolved six-line magnetic hyperfine pattern typical of effective internal field much larger than quadrupole splitting is observed.

The observed spectrum at room temperature of a quenched sample of β-$FeMoO_4$, containing less than 10% α phase by X-ray determination, is shown in Figure 3c. This is interpreted as two quadrupole split

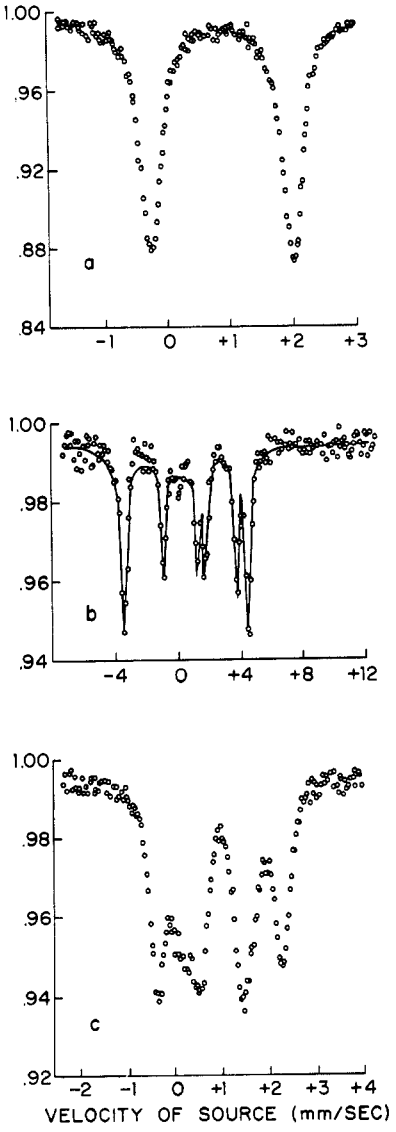

Figure 3.—Mössbauer effect of $FeMoO_4$: (a) $FeMoO_4$-II, 297°K, above Neel point; (b) $FeMoO_4$-II, 4.2°K, below Neel point; (c) β-$FeMoO_4$, 297°K.

pairs from the predominant β phase plus a small amount of the α-phase spectrum as background. Reducing the temperature of this sample resulted in spectra identical with those of α-$FeMoO_4$ at 78 and 4.2°K, thus showing that at 78°K the β phase has been completely converted to the α phase. This conclusion is verified by the observation of only the pure α-$FeMoO_4$ spectrum upon returning to room temperature.

The isomer shifts, quadrupole splittings, line widths, and effective internal fields from the above analyses are summarized in Table V. The quadrupole splittings and isomer shifts observed in all three phases are characteristic[20] of high-spin ferrous iron.

Electrical Resistivity.—Electrical measurements showed typical semiconducting behavior with an activation energy of about 0.15 eV for both α-$FeMoO_4$ and $FeMoO_4$-II. The resistivity at room temperature was 16 ohm-cm for $FeMoO_4$-II and about 76 ohm-cm for α-$FeMoO_4$.

(20) J. F. Duncan and R. M. Golding, *Quart. Rev.* (London), **19**, 36 (1965).

TABLE V

MÖSSBAUER-EFFECT PARAMETERS OF $FeMoO_4$

Phase	Temp, °K	ΔE_Q (±0.02), mm/sec	i.s.[a] (±0.02), mm/sec	$\Delta\nu$ (±0.1), mm/sec
β	297[b]	2.6[f]	0.9[f]	0.4
		0.9[f]	1.0[f]	0.4
α	297	1.52	0.86	0.4
	246	1.62	0.88	0.4
	78	1.93	0.88	0.5
	4.2[c]	2.65	0.90	0.7
		1.41	0.71	0.7
II	297	1.74	1.12	0.4
	78	1.75	1.36	0.5
	4.2[d]	1.77[e]	1.2[g]	0.4

[a] Isomer shifts relative to Fe^{57} in copper. [b] Alternate interpretation of observed four-line spectrum: ΔE_Q = 1.81, i.s. = 0.53; ΔE_Q = 1.74, i.s. = 1.36. [c] Alternate interpretation assuming magnetic order with $H \cong$ 35,000 Oe or assuming no order with ΔE_Q = 2.22, i.s. = 1.12; ΔE_Q = 1.84; i.s. = 0.50. [d] Magnetic ordered phase with H = 217,000 ± 3,000 Oe. [e] Assuming axial symmetric electric field gradient, with axis perpendicular to internal magnetic field. [f] Larger error range, ±0.1 mm/sec, due to greater uncertainty in the fitting of the spectrum. [g] Larger error, ±0.1 mm/sec.

Discussion

This investigation has revealed that there are at least three polymorphs of $FeMoO_4$. Contrary to many reports, all three forms appear to be known structure types. The failure of most previous investigators to note that α-$FeMoO_4$ is isotypic with $CoMoO_4$ and $NiMoO_4$ and that β-$FeMoO_4$ is isotypic with $MgMoO_4$ and $MnMoO_4$ is now readily understood. A mixture of α- and β-$FeMoO_4$ is easily obtained, and this mixture gives a very complex powder pattern that might appear to be triclinic.

The transformation of $FeMoO_4$-II to α-$FeMoO_4$ on heating is unusual in that it is endothermic. Since the transformation of an unstable phase to a stable phase is generally, but not necessarily, exothermic, one might expect that $FeMoO_4$-II is really the stable form of $FeMoO_4$ at STP. However, since α-$FeMoO_3$ may be prepared well below 600°, it would appear that α-$FeMoO_4$ is the stable form at STP.

Abrahams[10] has indicated that although $MnMoO_4$ and $CoMoO_4$ have the same space groups and similar cell dimensions, they are not isotypic. We have further shown this in that α-$FeMoO_4$ ($CoMoO_4$-type structure) does not transform smoothly to β-$FeMoO_4$ ($MnMoO_4$-type structure). The transition is abrupt, presumably first order, and the high-temperature form can be obtained at room temperature by quenching. Similar transformations can in fact be found for $NiMoO_4$ and $CoMoO_4$,[18] although β-$NiMoO_4$ and β-$CoMoO_4$ are much more difficult to obtain by quenching. In Table II the cell dimensions of all $AMoO_4$-type compounds isotypic with α- and β-$FeMoO_4$ are given. Most of the cell dimensions are listed for the first time. As may be seen, a β angle of about 114° is typical of α-$CoMoO_4$ isotypes while this angle is about 106° for $MnMoO_4$ isotypes. The interaxial ratios also distinguish quite well between the two structure types despite the similarity in their cell dimensions.

The arrangements of metal atoms in $MnMoO_4$ and $CoMoO_4$ are very similar, but the oxygen positions are considerably different. The most significant difference between the two structures is, as Abrahams[10] has pointed out, that the Mo to O coordination in $MnMoO_4$ is basically tetrahedral while in α-$CoMoO_4$ the Mo to O coordination is distorted octahedral. Although this difference in coordination might appear to be a matter of degree, this is apparently not the case. The two structures are clearly not isotypic, and it is apparently coincidental that they have the same space group and similar cell dimensions. The transformations between α and β types of $FeMoO_4$, $CoMoO_4$, and $NiMoO_4$ apparently center around a change in the coordination of Mo. This has previously been suggested[15] for $CoMoO_4$ and $NiMoO_4$.

There are two crystallographic kinds of Co and Mn in α-$CoMoO_4$ and $MnMoO_4$, respectively. In both structures one kind of A cation is on the mirror plane and the other is on the twofold axis. However, both kinds of A cation in both structures have such a similar, nearly octahedral coordination that it would not be surprising if the Mössbauer data of α- and β-$FeMoO_4$ did not distinguish between the two kinds of Fe present in each type. The observed Mössbauer results do not distinguish between the two kinds of Fe in α-$FeMoO_4$, but the two kinds are distinguished in β-$FeMoO_4$.

The magnetic susceptibility and Mössbauer effect studies establish the existence of high-spin Fe^{2+} in all three forms of $FeMoO_4$. Thus the basic valence combination in all phases must be $Fe^{2+}Mo^{6+}O_4$. The observed semiconducting behavior of α-$FeMoO_4$ and $FeMoO_4$-II also tends to rule out a delocalized electron associated with possible Mo^{5+}. The high-pressure phase orders antiferromagnetically below 45°K exhibiting an internal effective field of the order commonly observed for Fe^{2+} systems. The low-pressure and high-temperature phases are less well understood, but since in the Mössbauer effect the isomer shift is related to the total electron density at the nucleus exhibiting the effect and the quadrupole splitting measures the electric field gradient at that nucleus, a comparison of these parameters in the various phases might be of value.

The isomer shifts of the α-$FeMoO_4$ phase are clearly less than for the $FeMoO_4$-II phase indicating a higher s-electron density at the iron nucleus of the former. This could be due to a smaller interaction between the iron d orbitals and the filled oxygen orbitals in the low-pressure phase leading to a smaller effective number of d electrons on the metal.[21] This corresponds to less shielding of the s electrons by the d electrons and would result in the observed higher electron density in α-$FeMoO_4$. This postulated smaller metal–oxygen interaction is consistent with the view that α-$FeMoO_4$ does not show magnetic order whereas the $FeMoO_4$-II with its greater interaction does and is also consistent with the observation that α-$FeMoO_4$ is 14% less dense than $FeMoO_4$-II.

The temperature dependence of the quadrupole splitting for α-$FeMoO_4$ can be understood in two ways. First, the basic crystal structure is independent of temperature up to at least 400° where it transforms to the β phase, but the distortion from pure cubic symmetry removes the degeneracy of the t_{2g} orbitals. The high-spin Fe^{2+} in an approximately octahedral field can be viewed as a half-filled d shell contributing no net electric field gradient plus one extra electron in the t_{2g} set. For sufficiently large splitting within the t_{2g} set the population distribution of the electron giving rise to the gradient will be strongly temperature dependent because of the Boltzmann factor. Since the contribution to the gradient is not the same for all of the orbitals of the t_{2g} set,[22] this means that the observed electric field gradient would depend on temperature.

Second, the degree of distortion from perfect octahedral symmetry in the α-$FeMoO_4$ lattice may increase with decreasing temperature. In this view all iron sites are almost equivalent in terms of the Mössbauer effect at higher temperatures, but at liquid helium temperature two different iron sites are clearly evident. This distortion might be associated with a phase change at some lower temperature, which would account for the anomalous magnetic susceptibility.

The alternate view, that α-$FeMoO_4$ is antiferromagnetically ordered at liquid helium temperature as suggested by the magnetic susceptibility data, requires that the effective internal field ($H \leq 35{,}000$ Oe) from the Mössbauer effect be much smaller than usually observed.[23] Antiferromagnetism and a positive Weiss constant would be consistent if there were strong ferromagnetic interactions within a sublattice and weaker antiferromagnetic interactions between sublattices. This view, although possible, seems less likely. Similarly an explanation of the low-temperature susceptibility of α-$FeMoO_4$ on the basis of an equilibrium between low- and high-spin states for the iron seems unlikely in view of the large quadrupole splittings.

Less is known about the β phase. At room temperature its total paramagnetic susceptibility is of the same order of magnitude as the α and II phases. The Mössbauer data show at least two kinds of iron sites, both containing high-spin Fe^{2+}. The isomer shifts indicate electron densities at the iron nuclei intermediate between the other two phases, and the two quadrupole splittings suggest that the two sites differ greatly in degree of distortion from perfect octahedral symmetry.

Acknowledgments.—We wish to thank J. L. Gillson for the electrical resistivity measurements, C. L. Hoover and staff for experiments over 3 kbars, and H.S. Jarrett, W. H. Cloud, and C. T. Prewitt for helpful discussions.

(21) L. R. Walker, G. K. Wertheim, and V. Jaccarino, *Phys. Rev. Letters*, **6**, 98 (1961).

(22) G. K. Wertheim, "Mössbauer Effect," Academic Press Inc., New York, N. Y., 1964.

(23) R. E. Ingalls, Technical Reports 2 and 3, Carnegie Institute of Technology, Pittsburgh, Pa., 1963.